Theor Chim Acta (1986) 70: 153-163

Theoretica Chimica Acta

Dynamic electron transfers in B_2H_6 and $Cu(PH_3)_2(BH_4)$

Kenai Hori* and Akitomo Tachibana**

[1] Department of Chemistry, Faculty of Liberal Arts, Yamaguchi University, Yoshida, Yamaguchi, 753 Japan
[2] Department of Hydrocarbon Chemistry, Faculty of Engineering, Kyoto University, Sakyo-ku, Kyoto, 606 Japan

(Received November 7, 1985, revised and accepted May 20, 1986)

In order to investigate the coupling of molecular vibrations and electron distribution, dynamic electron transfers in B_2H_6 and $Cu(PH_3)_2(BH_4)$ are lated by using a new variational method. In both molecules, the dynamic electron density near bridging hydrogen atoms decreases to form the density valley by exciting specific vibrational modes. On the other hand, in both sides of the valley density hills grow up. For these molecules, similar contour maps are given by the modes with different symmetry which have large contribution of the bridging ligands. While the dynamic electron transfer of B_2H_6 arises in symmetric form, the vibrational modes of the Cu complex gives the asymmetric redistribution of the dynamic electron density. This is attributed to the difference of the symmetry between the two molecules.

Key words: Dynamic electron density — Dynamic electron transfer — Electron transfer reaction

1. Introduction

Chemical reactions with small activation energies are largely influenced by molecular vibration. This is because energies of vibrations are almost equal to or larger than barriers of reactions. The electron transfer in binuclear complexes is a typical reaction with such conditions [1]. In these kinds of reactions vibrational

* *Present address*: Department of Physiology and Biophysics, Mount Sinai School of Medicine of the City University of New York, NY 10029, USA
** Also belongs to Division of Molecular Engineering, Graduate School of Engineering, Kyoto University

modes can be divided into two categories [2]. One is the bath mode which works as the energy lifting function throughout the chemical reaction. The other is the mode which largely concerns with a specific reaction and is called the system mode. For example, in the case of binuclear complexes some vibration modes including the motion of bridging ligands will act as the system mode of the ligand in the electron transfer processes.

In the previous papers [3], we developed a new variational method which includes operator for kinetic energy of nuclei in Hamiltonian. The method can give the dynamic electron density, that is, the electron density which includes the effect of molecular vibration. The redistribution of the electron density which is called the dynamic electron transfer can be also estimated. Therefore, it is expected that the new method will give more information that cannot be given by other methods.

In this paper, we calculated dynamic electron transfers of B_2H_6 and $Cu(PH_3)_2(BH_4)$ molecules. B_2H_6 has two boron atoms bridged by two ligand hydrogens similar to those in the Cu complex. These bridging ligands are members of the BH_4^- fragment in both molecules. Therefore, BH_4^- is considered to coordinate to remaining BH_2^+ and $[Cu(PH_3)_2]^+$ fragments. While the former fragments has only *s*- and *p*-orbitals, the metal moiety of the latter has not only them but *d*-orbitals which have relatively flexible electrons. Therefore, it is very interesting to investigate and compare the dynamic electron transfers in these molecules. Calculations of their dynamic property will help better understanding of the relation between the electron-phonon coupling and the electron or ligand transfer reactions of transition metal complexes.

2. Method of calculation

In this section, we will show the brief outline of the variational method which includes the dynamic effect of molecules. The total Hamiltonian includes the electron and nuclear motions, He and T_{nuc}, as follows:

$$H = \text{He} + T_{\text{nuc}}, \tag{1}$$

where

$$T_{\text{nuc}} = -\sum_{\alpha} 1/2(\partial/\partial Q\alpha)^2. \tag{2}$$

In this expression, $Q\alpha$ denotes the αth normal coordinate of molecular vibration. The total wave function is given as the product of the wave function of electron, Ψe, and that of nuclei Ψ_{nuc},

$$\Psi = \Psi e \Psi_{\text{nuc}}. \tag{3}$$

In the closed shell system, Ψe can be obtained by solving the dynamic Fock equation as follows [3]:

$$f_{rs} = \langle h_{rs} \rangle_{\text{nuc}} + \left\langle \sum_{j}^{\text{occ}} \sum_{t,u} C_{tj} C_{uj} \{2(rs|tu) - (rt|su)\} \right\rangle_{\text{nuc}} + \sum_{\alpha} \langle \Delta_{rs}; \alpha \rangle_{nuc}, \tag{4a}$$

and

$$\Delta_{rs};\ \alpha = 1/2\langle \partial\psi_r/\partial Q\alpha | \partial\psi_s/\partial Q\alpha\rangle - 1/2 \sum_{j}^{\text{occ}} \sum_{t,u} C_{tj}C_{uj}\{\langle \partial\psi_r/\partial Q\alpha|\psi_t\rangle\langle \partial\psi_s/\partial Q\alpha|\psi_u\rangle + \langle \partial\psi_t/\partial Q\alpha|\psi_r\rangle\langle \partial\psi_u/\partial Q\alpha|\psi_s\rangle\}, \tag{4b}$$

where $\{\psi_r\}$ is the orthonormal basis set and the orbitals are assumed to be real. $\langle F\rangle_{\text{nuc}}$ indicates that the operator F is averaged with respect to the nuclear wave function.

The dynamic electron density is given as follows

$$\langle\rho\rangle n = \langle \Psi^*_{n:\text{nuc}}|\rho|\Psi_{n:\text{nuc}}\rangle, \tag{5}$$

where n denotes the vibrational quantum number. The dynamic electron transfer is defined as the difference between $\langle\rho\rangle n$ and $\langle\rho\rangle_0$:

$$\Delta\langle\rho\rangle n = \langle\rho\rangle n - \langle\rho\rangle_0. \tag{6}$$

This represents the redistribution of the dynamic electron density induced by excitation of the molecular vibration.

In the previous papers [3], we proved that the dynamic electron density satisfies the additive property if we adopt the harmonic wave function as $\Psi_{n:\text{nuc}}$, i.e.

$$\langle\rho\rangle n \sim \rho(0) + (1/2\omega)(\partial^2\rho/\partial Q^2)(0)(n+1/2), \tag{7}$$

where ω is the vibrational frequency. In order to obtain Eq. (7), we expressed ρ in terms of a Taylor series expansion with respect to the normal coordinate,

$$\rho(Q) \sim \rho(0) + (\partial\rho/\partial Q)(0) + (1/2)(\partial^2\rho/\partial Q^2)(0)Q^2. \tag{8}$$

Equation (7) shows that the difference between the dynamic electron densities with quantum numbers $n+1$ and n is expressed by

$$\langle\rho\rangle n+1 \sim \langle\rho\rangle n + \Delta\langle\rho\rangle, \tag{9}$$

where

$$\Delta\langle\rho\rangle = (1/2\omega)(\partial^2\rho/\partial Q^2)(0) \tag{10}$$

Using Eq. (9), Eq. (6) is reduced to

$$\Delta\langle\rho\rangle n \sim n\Delta\langle\rho\rangle \qquad (n = 1, 2, 3, \ldots). \tag{11}$$

The zero-point vibration itself brings about half of $\Delta\langle\rho\rangle_1$ over the static electron density:

$$\Delta\langle\rho\rangle_{00} \sim 1/2\Delta\langle\rho\rangle_1, \tag{12}$$

where

$$\Delta\langle\rho\rangle_{00} = \langle\rho\rangle_0 - \rho(0). \tag{13}$$

It should be noted that the contribution of Δ_{rs}; α in Eq. (4) is considered to be smaller than the other terms. If Δ_{rs}; α is neglected, ρ is identical to the adiabatic electron density. We adopted this simplification in the present calculations and used the numerical integration technique in order to obtain the dynamic electron density.

MO calculations are carried out by use of the GAUSSIAN-80 program [4]. Subroutines are added in order to calculate the dynamic electron density and dynamic electron transfer. For calculation of the transition metal complexes, the basis sets of Cu given by Roos et al. are contracted to [5s2pld] and *p*- and *d*-type orbital of $1G$ ($\zeta = 0.25$ and 0.1682, respectively) are added to the basis set [5]. Those for *B* and bridging *H* are the 3-21G basis sets internal to the program [6]. For the other ligand atoms coordinating to Cu and *B*, STO-3G minimal basis sets [7] were used for the sake of computational time. 3-21G basis sets are used for all atoms of B_2H_6. Geometries of molecules are optimized using the energy gradient method. The second derivatives of the potential energy are obtained by the numerical differentiation of the analytically calculated energy gradient.

3. Results and discussion

3.1. Dynamic electron transfer in B_2H_6

Motions of bridging ligands play an important role in the electron transfer reactions. In the present calculations, therefore, we choose two modes with $\nu_1 = 1820.6$ and $\nu_2 = 1915.2\ \mathrm{cm}^{-1}$ as shown in Fig. 1. In both modes the motions of the bridging ligands have the main contribution of the normal coordinates.

Table 1 summarizes $\Delta\langle\rho\rangle_{00}$ and $\Delta\langle\rho\rangle_1$ of B_2H_6 along the lines $y = 1.7$ and 0.0 au in the *xy*-plane. The units of coordinates and electron density are in au and e/au^3, respectively, throughout this paper. Positive and negative dynamic electron transfers indicate increase and decrease of the dynamic electron density, respectively. The ratios defined as $\Delta\langle\rho\rangle_1/\Delta\langle\rho\rangle_{00}$ on the former line are in the range of 1.949 to 2.012 except for the point with $x = 0.2$. This trend is consistent with the theoretical value 2.0 as given by Eq. (12). On the other hand, the ratios on the

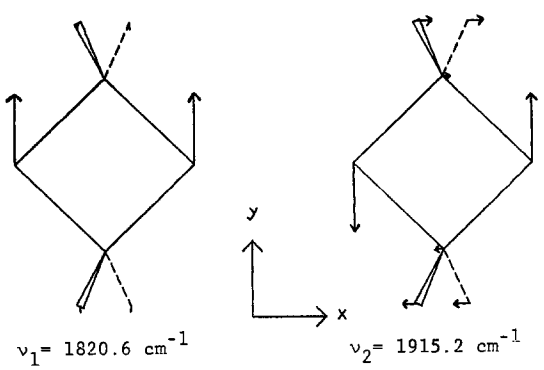

Fig. 1. Vibrational modes of B_2H_6 for the calculation of the dynamic electron transfer. *Arrows* show the vector of vibration

Table 1. Comparison of $\Delta\langle\rho\rangle_1$ and $\Delta\langle\rho\rangle_{00}$ calculated for B_2H_6

x-coordinate[1]	$y = 1.7$ au $\Delta\langle\rho\rangle_0{}^2$	$\Delta\langle\rho\rangle_1{}^2$	Ratio[3]	$y = 0.0$ au $\Delta\langle\rho\rangle_0{}^2$	$\Delta\langle\rho\rangle_1{}^2$	Ratio[3]
0.0	0.011631	0.023403	2.012	−0.000074	−0.000142	1.919
0.2	−0.000192	−0.000315	1.641	−0.000131	−0.000252	1.924
0.4	0.000100	0.000200	2.000	−0.000306	−0.000593	1.937
0.6	0.000495	0.000495	1.949	−0.000609	−0.001184	1.944
0.8	0.000350	0.000692	1.977	−0.001072	−0.002077	1.938
1.0	0.000422	0.000843	1.998	−0.001864	−0.003567	1.914
1.2	0.000481	0.000962	2.000	−0.003706	−0.006898	1.861
1.4	0.000519	0.001042	2.008	−0.008202	−0.014786	1.803
1.6	0.000527	0.001059	2.009	−0.015757	−0.027773	1.763
1.8	0.000498	0.001001	2.010	−0.020705	−0.036158	1.746

[1] In au unit
[2] In e/au[3]
[3] Value of $\Delta\langle\rho\rangle_1/\Delta\langle\rho\rangle_{00}$

Table 2. Dynamic electron transfers and their ratios calculated for B_2H_6

x-coordinate[1]	$y = 1.7$[1] $\Delta\langle\rho\rangle_2{}^2$	$\Delta\langle\rho\rangle_3{}^2$	$y = 0.0$[1] $\Delta\langle\rho\rangle_2{}^2$	$\Delta\langle\rho\rangle_3{}^2$
0.0	0.046757	0.70004	−0.000257	−0.000347
	(1.998)[3]	(2.991)	(1.810)	(2.444)
0.2	−0.000627	−0.000938	−0.000473	−0.000665
	(1.990)	(2.978)	(1.887)	(2.639)
0.4	0.000402	0.000606	−0.001139	−0.001640
	(2.010)	(3.030)	(1.921)	(2.766)
0.6	0.000995	0.001499	−0.002291	−0.003324
	(2.010)	(3.028)	(1.935)	(2.807)
0.8	0.001392	0.002098	−0.004020	−0.005837
	(2.012)	(3.032)	(1.935)	(2.810)
1.0	0.001697	0.002561	−0.006833	−0.009838
	(2.013)	(3.038)	(.916)	(2.758)
1.2	0.001941	0.002932	−0.012883	−0.018148
	(2.018)	(3.048)	(1.868)	(2.631)
1.4	0.002105	0.003185	−0.026787	−0.036745
	(2.020)	(3.057)	(1.811)	(2.485)
1.6	0.002143	0.003245	−0.049233	−0.066270
	(2.024)	(3.064)	(1.773)	(2.386)
1.8	0.020026	0.003072	−0.063517	−0.084836
	(2.024)	(3.069)	(1.757)	(2.346)

[1] In au unit
[2] In e/au[3]
[3] Values of parenthese are ratios defined as $\Delta\langle\rho\rangle n/\Delta\langle\rho\rangle_1$

latter line are small in comparison with the theoretical value, especially, at the points with x-coordinates larger than 1.2.

$\Delta\langle\rho\rangle_2$, $\Delta\langle\rho\rangle_3$ and ratios defined by $\Delta\langle\rho\rangle_n/\Delta\langle\rho\rangle_1$ are listed in Table 2. While ratios on line the $y=1.7$ are almost equal to the theoretical values 2.0 and 3.0 for $\Delta\langle\rho\rangle_2$ and $\Delta\langle\rho\rangle_3$ as given by eq. (11), respectively, those of the line $y=0.0$ are smaller than the corresponding theoretical values. This is similar to that seen in Table 1. It should be noted that the bridging hydrogen atom lines at a point on the line (1.824, 0.0) and largely moves by the molecular vibrations. These results indicate that almost everywhere the numerical values of the dynamic electron transfers with higher quantum numbers are roughly estimated by Eq. (11). However, they are overestimated at points near the atoms which have large contribution to the molecular vibration. For these points, Eq. (8) is not a good approximation for estimation of the dynamic electron density. It is necessary to consider the unharmonicity of the electron density in order to explain such a deviation. The similar results are also obtained for dynamic electron transfers of the Cu complex.

The dynamic electron transfer with $n=3$, $\Delta\langle\rho\rangle_3$, induced by modes 1 and 2 in the xy-plane are shown in Fig 2a, b, respectively. Both figures display that the density valley is formed near the hydrogen atom which largely moves due to the harmonic oscillation of the molecule. On the other hand, hills of the dynamic electron transfer come to arise in both sides of the density valley. Although the two modes have different symmetry, the dynamic electron transfer induced by the mode 1 (Fig. 2a) very much resembles that by the mode 2 (Fig. 2b). It is very interesting that the different vibrations give similar contours.

Figure 3a displays the dynamic electron transfer on the yz-plane induced by the mode 1. The decrease of the electron density near terminal hydrogens are small in comparison with that near the bridging hydrogen. This is attributed to the fact that the main contribution of the normal coordinate is the motion of the latter atom. Figure 3b displays the contour on the plane which is parallel to the yz-plane at $x=1.824$ au. The bridging hydrogen atom lies at the bottom of the valley in this figure. The decrease of the dynamic electron density occurs considerably in the upper region of the ligand. In Fig. 2a, the region of the negative transfer also spreads along the x-axis. These figures suggests that the electron density is transferred from s-orbital of the hydrogen atom.

As mentioned above, the contribution of the displacement vector in the system mode determines the depth of the density valley and the height of the density hill. The deepest region of the valley exists near the ligand hydrogen atom. For example, in Fig. 2a $\langle\rho\rangle_0$ and $\Delta\langle\rho\rangle_3$ of the point at which a bridging hydrogen lies are calculated to be 0.351219 and -0.084836, respectively. Moreover, around this point there is a circle of the negative transfer with the contour value of -0.03 (-6). The dynamic electron transfer which corresponds to 20–30% of $\langle\rho\rangle_0$ occurs. On the other hand, the highest points of the hills are in both sides of the valley. Values of $\langle\rho\rangle_0$ and $\langle\rho\rangle_3$ at the point are calculated to be 0.159216 and 0.027089, respectively.

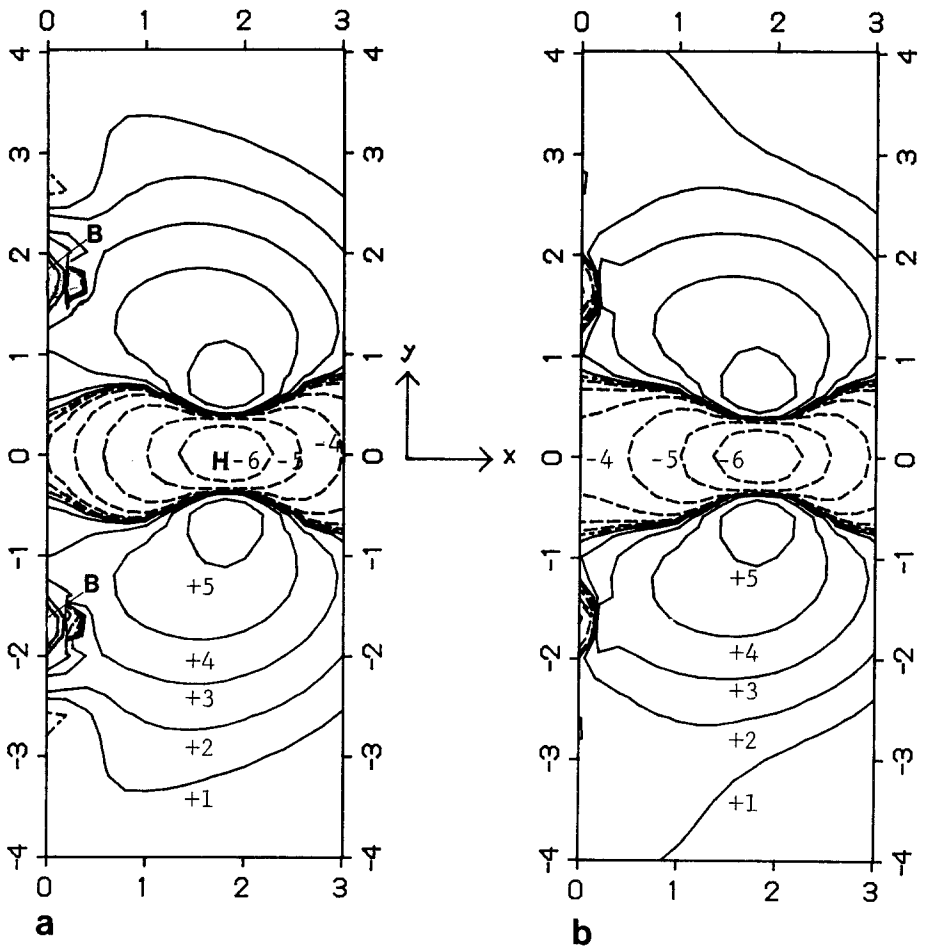

Fig. 2ab. Dynamic electron transfers of B_2H_6 with $n = 3$ on the xy-plane. **a** and **b** are contours induced by modes 1 and 2, respectively. Indexes 0, ±1, ±2, ±3, ±4, ±5, and ±6 means magnitude of dynamic electron transfers which correspond to the height 0.0, ±0.0001, ±0.0003, ±0.001, ±0.003, ±0.01 and ±0.03, respectively

3.2. *Dynamic electron transfer of $Cu(PH_3)_2(BH_4)$*

Two possible geometries are considered for the Cu complex. They are tetrahedral and square planer structures, 1 and 2, respectively. Optimized values of bond lengths and angles for geometrical isomers are listed in Table 3 together with those observed in $Cu(PPh_3)_2(BH_4)$ [8].

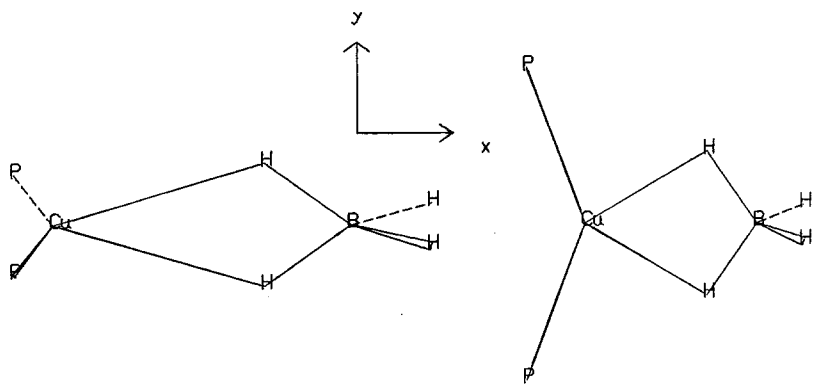

1 2

Table 3. Optimized parameters[1] of $Cu(PH_3)_2(BH_4)$ with tetrahedral 1 and square planar 2 geometries

	1	2	Exp[2]
CuP	2.345	2.394	2.276
CUB	2.470	2.445	2.184
CuH_1[3]	2.036	2.018	2.02
BH_1[3]	1.256	1.254	1.26
BH_2[3]	1.210	1.209	1.37
∠BCuP	98.0	110.5	118.4

[1] Units of bond lengths and angles are Å and degree, respectively

[2] See [8]

[3] H_1 and H_2 designate bridging and terminal hydrogens in the BH_4^- fragment, respectively

Total energies of 1 and 2 are calculated to be −2340.59065 and −2340.58394 au, respectively. 1 is more stable by 0.0067 au (4.2 kcal/mol) than 2. The X-ray crystallographic data indicated that the complex has the tetrahedral geometry [8]. Cu-H_1 and B-H_1 lengths calculated are in good agreement with those observed. Cu-B and Cu-P lengths are overestimated by 0.286 and 0.069 A, respectively. Optimized values of the B-H_2 length and the BCuP angle are underestimated by 0.160 A and 20.4°, respectively. These trends are attributed to the difference of the ligands, PH_3 and PPh_3, and/or the insufficient basis sets for P and H atoms in the PH_3 ligand.

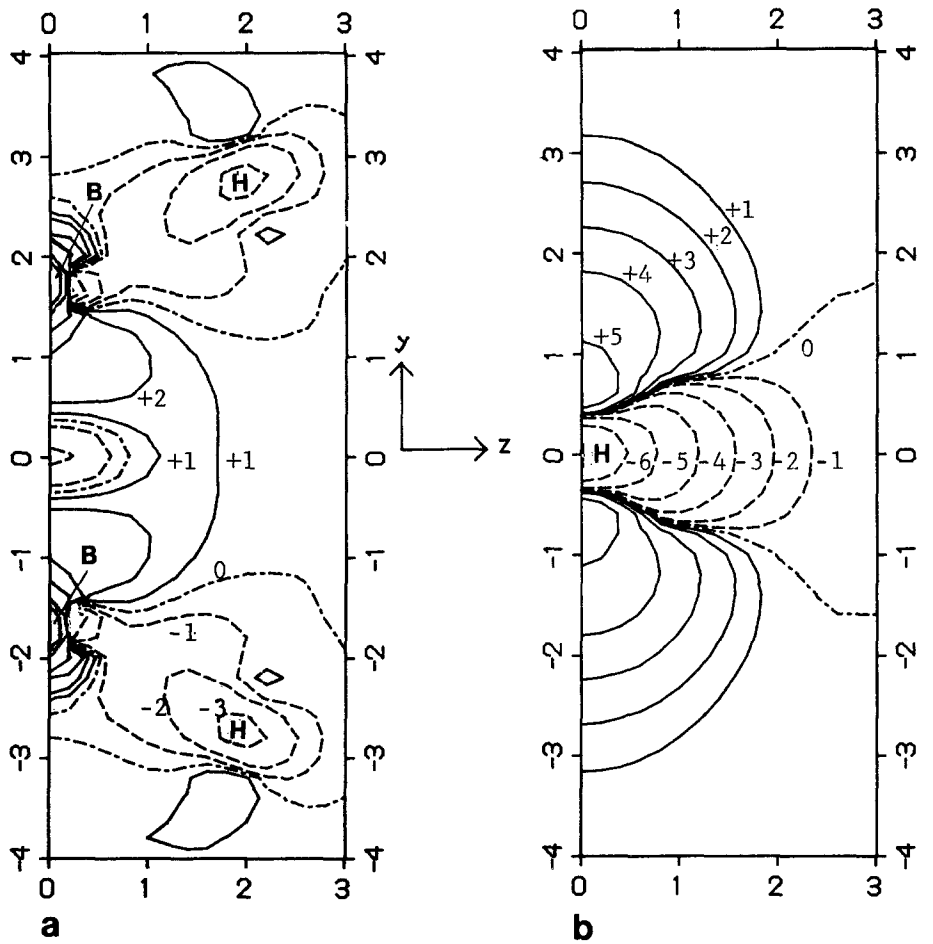

Fig. 3ab. Dynamic electron transfer of B_2H_6 with $n = 3$ induced by the mode 1. **a** and **b** are contours on the *yz*-plane and on the plane which is parallel to the *yz*-plane at $x = 1.824$, respectively. Indexes in these figures are identical with those in Fig. 2

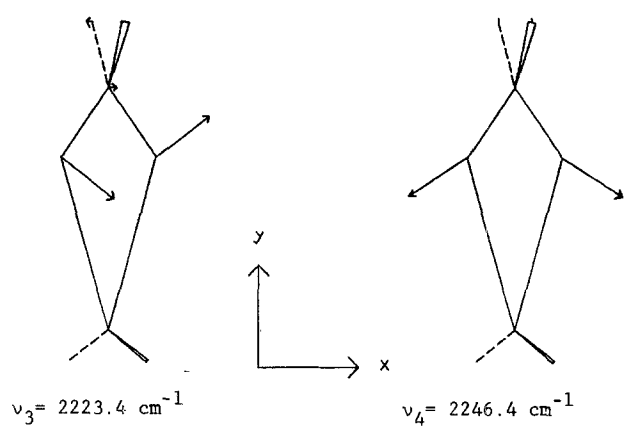

Fig. 4. Vibrational modes of $Cu(PH_3)_2(BH_4)$ for the calculation of the dynamic electron transfer. *Arrows* show the vector of vibration

The second derivative calculation of 1 gives one negative frequency with 68i cm^{-1}. Three imaginary frequencies are also calculated for 2. The first mode with the frequency 729.0i cm^{-1} is the mode that causes its geometry change to tetrahedral structures. The second with the frequency 158i cm^{-1} leads to coordination of the third hydrogen to the copper atom. The last is the mode with the frequency 39i cm^{-1}. However, the imaginary modes with frequencies 68i and 39i cm^{-1} may be artificial because the numerical second derivative calculation does not have precision for small frequencies, especially such large molecule as calculated in the present work.

Figure 4 displays the modes 3 and 4 with frequencies $\nu_3 = 2223.4$ and $\nu_4 = 2246.4$ cm^{-1}, respectively, used for the calculation of the dynamic electron transfers in $Cu(PH_3)_2(BH_4)$. Both modes have large contribution of the motion of

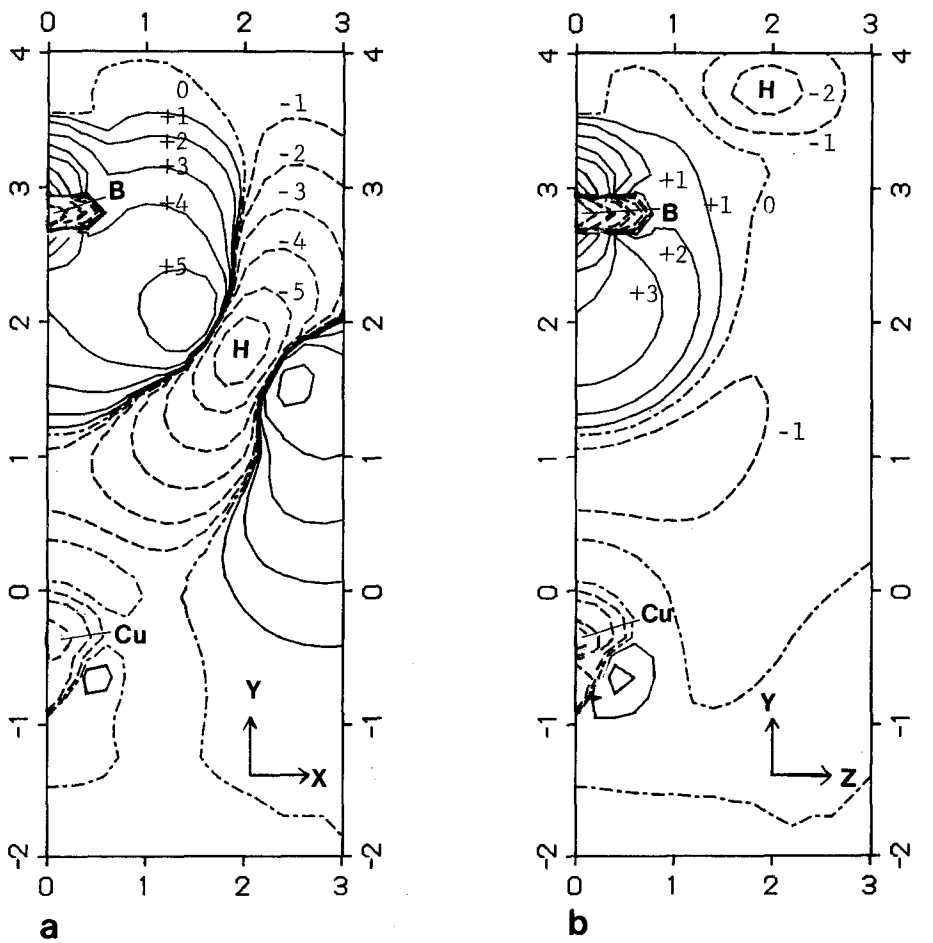

Fig. 5ab. Dynamic electron transfers of the Cu complex with $n = 3$ induced by mode 3. **a** and **b** are contours on the *xy*- and *yz*-planes, respectively. Indexes in these figures are identical with those in Fig. 2

bridging hydrogen atoms similar to modes 1 and 2 of B_2H_6. The B_2H_6 molecule arranges its atoms symmetric against the axis constructed with the bridging two hydrogen ligands. This geometrical feature leads to the symmetric dynamic electron transfer in Fig. 2. On the other hand, in the case of the Cu complex the dynamic electron transfer is expected to be asymmetric because of the absence of such an axis.

Figure 5a, b show the dynamic electron transfers on *xy*- and *yz*-planes induced by the mode 3, respectively. Figure 5a shows that the harmonic oscillation of the molecule also makes the density valley near the hydrogen ligand. The loss of the electron density of the ligand results in the appearance of the hill between boron and hydrogen atoms. The density hill also appears in the other site of the density. In this figure, there are contour lines with -6 (-0.03) and $+5$ (0.01) for the valley and the hill. Similar contours are also obtained by the excitation of the other normal mode 4. These characters are the same as those obtained for B_2H_6.

There is a distinct difference between the dynamic electron transfers of molecules with and without the transition metal fragment. It is the asymmetry of the dynamic electron transfer seen in Fig. 5a. That is, the dynamic electron transfer mainly arises near the BH_4^- fragment. Since the hydrogen ligand has only one electron, the absolute value of dynamic electron transfers is not so large. However, the excitation of a specific molecular vibration causes the different and asymmetric redistribution of the electron density in metal and boron fragments. While this effect does not directly concern with the electron transfer reaction, this trend of the dynamic electron transfer gives important information for the redox reactions.

Acknowledgement. Permission to use FACOM M-382 and VP-100 Computers at Data Processing Center of Kyoto University is gratefully acknowledged. The authors also thank the Computer Center, Institute for Molecular Science, for the use of HITAC M-200H Computer. The work was carried out by a Grant-in-Aid from the Ministry of Education of Japan.

References and notes

1. Basolo F, Pearson RG (1967) Mechanism of inorganic reaction. Wiley, New York
2. Miller WH (1981) In: Truhlar GD (ed) Potential energy surface and dynamic calculations. Plenum, New York
3. (a) Tachibana A, Hori K, Asai Y, Yamabe T, (1984) Chem Phys Lett 106: 36; (b) Tachibana A, Hori K, Asai Y, Yamabe T (1984) J Chem Phys 80:6170; (c) Tachibana A, Asai Y, Kohno M, Hori K, Yamabe T, (1985) ibid 83:6334; (d) Tachibana A, Hori K, Asai Y, Yamabe T, Fukui K (1985) J Mol Struct Theochem 123:267
4. Binkley JS, Whiteside RA, Krishnan R, Seeger R, DeFrees DJ, Schlegel HB, Topiol S, Kahn LR, Pople JA (1981) Quantum Chemistry Program Exchange 11:406
5. (a) Roos B, Veillard A, Vinot G (1971) Theor Chim Acta 20:1 (b) Hay PJ (1977) J Chem Phys 60 (c) Jensen JR, Fenske RF (1978) Theor Chim Acta 48:241
6. Hehre W, Stewart RF, Pople JA (1969) J Chem Phys 51:2657
7. Binkley JS, Pople JA, Hehre WJ (1980) J Am Chem Soc 102:939
8. Lippard SJ, Melmed KM (1976) Inorg Chem 6:2223